UC San Diego
UC San Diego Previously Published Works

Title
Digital Histological Study of Neocortical Grey and White Matter Tau Burden Across Tauopathies.

Permalink
https://escholarship.org/uc/item/55c1859c

Journal
Journal of Neuropathology and Experimental Neurology, 81(12)

Authors
Hiniker, Annie
Peterson, Claire
Kim, Yongya
et al.

Publication Date
2022-11-16

DOI
10.1093/jnen/nlac094

Peer reviewed

OXFORD

ORIGINAL ARTICLE

Digital Histological Study of Neocortical Grey and White Matter Tau Burden Across Tauopathies

David G. Coughlin (iD), MD, MTR, Annie Hiniker (iD), MD, PhD, Claire Peterson (iD), BSc,
Yongya Kim, Sanaz Arezoumandan (iD), MD, Lucia Giannini (iD), MD, Donald Pizzo, PhD,
Daniel Weintraub, MD, Andrew Siderowf, MD, MSCE, Irene Litvan (iD), MD,
Robert A. Rissman (iD), PhD, Douglas Galasko, MD, Lawrence, Hansen, MD, PhD,
John Q. Trojanowski, MD, PhD, Edward Lee (iD), MD, PhD, Murray Grossman, MD, and
David Irwin (iD), MD, MTR

Abstract

3R/4R-tau species are found in Alzheimer disease (AD) and ~50% of Lewy body dementias at autopsy (LBD+tau); 4R-tau accumulations are found in progressive supranuclear palsy (PSP) and corticobasal degeneration (CBD). Digital image analysis techniques can elucidate patterns of tau pathology more precisely than traditional methods but repeatability across centers is unclear. We calculated regional percentage areas occupied by tau pathological inclusions from the middle frontal cortex (MFC), superior temporal cortex (STC), and angular gyrus (ANG) from cases from the University of Pennsylvania and the University of California San Diego with AD, LBD+tau, PSP, or CBD (n = 150) using QuPath. In both cohorts, AD and LBD+tau had the highest grey and white matter tau burden in the STC (p ≤ 0.04). White matter tau burden was relatively higher in 4R-tauopathies than 3R/4R-tauopathies (p < 0.003). Grey and white matter tau were correlated in all diseases (R^2=0.43–0.79, p < 0.04) with the greatest increase of white matter per unit grey matter tau observed in PSP (p < 0.02 both cohorts). Grey matter tau negatively correlated with MMSE in AD and LBD+tau (r = −4.4 to −5.4, p ≤ 0.02). These data demonstrate the feasibility of cross-institutional digital histology studies that generate finely grained measurements of pathology which can be used to support biomarker development and models of disease progression.

Key Words: Alzheimer disease, Corticobasal degeneration, Dementia with Lewy bodies, Digital histology, Neuropathology, Progressive supranuclear palsy, Tau.

INTRODUCTION

Alzheimer disease (AD), Lewy body diseases ([LBD]: Parkinson disease [PD] and dementia with Lewy bodies [DLB]), progressive supranuclear palsy (PSP), and corticobasal degeneration (CBD) are heterogeneous disorders and definitive diagnosis is obtained only upon postmortem examination at autopsy (1–4). While 3R/4R tau accumulations in neurofibrillary tangles are a defining feature of AD and 4R tau species are a defining pathological feature of PSP and CBD, AD-related 3R/4R tau copathology is also commonly observed in LBD cohorts at autopsy in approximately 30%–50% of PD with dementia patients and 70% or more of patients with DLB (5–11). The presence of AD-related tau co-pathology has been related to faster time to dementia in PD, overall decreased survival in LBD, and altered motor, neuropsychiatric, and cognitive phenotypes (5, 6, 12–21). Moreover, the presence of co-occurring AD-related pathology decreases the likelihood of patients with DLB exhibiting core features of visual hallucinations, making diagnosis of mixed features more difficult (22). Some clinical syndromes are highly specific for particular pathologies, such as Richardson syndrome for PSP 4R tauopathy and amnestic AD for 3R/4R

tauopathy of AD (3). However, other pathologies like PSP and CBD tauopathy may present with other clinical phenotypes including PSP-CBD overlap syndromes, frontal presentations of behavioral variant FTD, and nonfluent or atypical variants of primary progressive aphasia (3, 23). Tau-directed positron emission tomography offers the potential ability to observe the presence and distribution of tau pathology during life (24), with initial tracers having more affinity for 3R/4R tau species but with second generation tracers showing greater promise for use in 4R tauopathies (25–34).

Detailed neuropathologic study of postmortem brain tissue can elucidate disease-specific patterns of tau pathology that may be useful to the continued development of imaging biomarkers. Indeed, PSP and CBD tauopathy has considerable white matter tau pathology in glia and axonal threads. Study of in vivo white matter connectivity using diffusion tensor imaging suggests white matter degeneration in PSP and CBD, which in comparative studies, is more severe than that in LBD (35, 36). However, dedicated studies of white matter histology in these disorders are rare. Additionally, standard neuropathological assessments using ordinal semiquantitative scores may have limited statistical power for comparative studies (37–40). Histological assessments using digital image analysis techniques offer the potential for greater objective measurements on a continuous spectrum with a greater dynamic range; while prior studies have shown excellent correlations of digital measurements and semiquantitative ordinal scores and manual counts, it has not been definitively shown that such approaches reliably scale to multicentered studies in which there may be methodological differences in tissue processing and immunohistochemical techniques between labs (41–49).

Here we use validated digital histological techniques in 2 autopsy cohorts from the University of Pennsylvania and the University of California San Diego to test the hypothesis that PSP and CBD tauopathies have greater relative cortical white matter tau compared to AD and LBD with co-occurring AD tauopathy (LBD+tau).

MATERIALS AND METHODS

Participants

From the University of Pennsylvania (UPenn), participant's data were obtained from UPenn Integrated Neurodegenerative Disease Database (50). Patients selected were clinically evaluated and followed at the UPenn Parkinson's disease and Movement Disorder Clinic, Frontotemporal Dementia Center, Alzheimer's disease Core Center, or the Michael J. Crescenz VA Medical Center's Parkinson's Disease Research, Education, and Clinical Center. From the University of California San Diego (UCSD), participants and data were abstracted from the UCSD Shiley Marcos Alzheimer's Disease Research Center (UCSD-ADRC) and their accompanying database. Patients were clinically evaluated and followed at the UCSD-ADRC, UCSD memory disorders clinic, and or the UCSD Parkinson's Disease and other Movement Disorders Center.

UPenn and UCSD autopsies were performed using similar standardized tissue sampling and processing protocols,

including fixation in 10% neutral buffered formalin and tissue processing (51, 52).

Expert neuropathologists at each institution (EL, JQT, LH, AH) applied current diagnostic criteria to assign Thal phases (53), Braak tau stages (37), CERAD neuritic plaque stages (54), α-synuclein Lewy body stages (55), the presence of TDP-43 (56), and aging-related tau astrogliopathy (ARTAG) copathology (57) at the time of autopsy. Final neuropathology diagnosis for each case was rendered using standard semiquantitative assessments for each pathology in each brain region (58). All procedures were performed with prior informed consent in accordance with UPenn and UCSD Institutional Review Board guidelines. Cases were selected that had available digital pathology images and either: 1) met clinical criteria for amnestic AD or amnestic MCI with autopsy conformation of intermediate or high degree of AD neuropathological change (58), 2) met clinical criteria for Lewy body dementia (PD dementia [59] or DLB [22]) with autopsy confirmation of LBD synucleinopathy (limbic/transitional or neocortical/diffuse stage [55]) and accompanying moderate to high levels of AD-related tau copathology (Braak stage III/VI and above [37]: LBD+tau), 3) met clinical criteria for PSP (either PSP-Richardson syndrome or a phenotype known to be associated with PSP pathology) (3) with autopsy confirmation of PSP tauopathy (60), or 4) met clinical criteria for an FTD-spectrum phenotype associated with CBD pathology with autopsy confirmation (4, 61). For the PSP and CBD groups, subjects with intermediate or high degrees of AD neuropathological change were excluded for the primary reason that differentiating AD-related tau pathology and PSP-related tau pathology by the applied digital methodologies is not currently possible (58). Cases with other secondary neuropathologic diagnoses were excluded (MSA, TDP-43, ARTAG, AGD, severe CVD). The selection criteria above yielded 36 AD, 20 LBD+tau, 23 PSP, and 10 CBD cases from UPenn and 21 AD, 16 LBD+tau, 17 PSP, and 7 CBD cases from UCSD for study (Table).

Digital Histology

Six-micrometer-thick sections from formalin-fixed paraffin-embedded sections from middle frontal cortex (MFC), superior temporal cortex (STC), and the angular gyrus (ANG) were immunostained for phospho-tau (AT8, Thermofisher MN1020). Regions were selected that were most consistently sampled across sites with the most available samples available for analysis. Primary antibody concentration and antigen retrieval methods were optimized per center (UPenn Digital Pathology Lab: 1:1000, no antigen retrieval. UCSD: 1:500, formic acid antigen retrieval). The immunohistochemistry protocols were performed at each laboratory were otherwise identical (see Supplementary Data). Digital images of histology slides were taken at 20× magnification (UPenn: Lamina slide scanning system PerkinElmer [Waltham MA], .mrxs file type. UCSD: Zeiss AxioScan Z1, [Oberkochen Germany], .czi file type). Pixel size of 6.5 μm^2 (i.e. pixel resolution of 0.325 μm), camera resolution of 2560×2160, and a bit depth of 16 was the same with both devices.

TABLE. Case Characteristics

	UPenn				UCSD			
	AD (n = 36)	LBD+Tau (n = 20)	PSP (n = 23)	CBD (n = 10)	AD (n = 21)	LBD+Tau (n = 16)	PSP (n = 17)	CBD (n = 7)
Clinical phenotype	Possible AD: 1 Probable AD: 35	DLB: 12 PDD: 8	PSP-RS: 13 PSP-P: 1 PSP-F: 5 PSP-SL: 3 PSP-CBS: 1	CBS: 3 PPA: 4 bvFTD: 2 PSP: 1	Probable AD: 20 MCI: 1	DLB: 11 PDD: 5	PSP-RS: 10 PSP-P: 2 PSP-F: 2 PSP-CBS: 1 Unknown: 2	Possible AD: 1 CBS: 3 PSP: 1 bvFTD: 2
Sex	Male 16 Female 20	Male: 15 Female: 5	Male: 16 Female: 7	Male: 5 Female: 5	Male: 7 Female: 14	Male: 11 Female: 5	Male: 11 Female: 6	Male: 2 Female: 5
Age at death, years (SD)**	76.8 (8.9)*	78.4 (6.1)	76.6 (6.5)	64.3 (8.7)	82.5 (12.3)	78.0 (7.2)	N=15, 76.5 (7.2)	73.3 (9.6)
Disease duration, years (SD)** ,***	10.5 (4.6)	9.7 (6.4)	7.4 (3.3)	N=9, 6.6 (2.9)	N=18, 12.2 (5.6)	7.3 (3.1)	N=16, 7.6 (5.4)	5.0 (4.6)
Brain weight, grams (SD)** ,***	1134 (147)	1327 (131)	1213 (129)*	N=9, 1088 (101)	1116 (262)	1258 (130)	N=14, 1217 (160)	1018 (117)
Postmortem interval, hours (SD)	12.6 (8.5)*	16.0 (8.8)*	11.2 (6.5)	N=9, 13.5 (7.5)	N=20, 6.1 (7.0)	N=13, 9.9 (6.7)	N=11, 8.7 (7.8)	N=6, 10.0 (3.9)
NIA-AA criteria[a]	Intermediate: 1 High: 35*	Intermediate: 11 High: 9	Not: 11 Low: 12 None: 23	Not: 4 Low: 6 None: 10	Intermediate: 5 High: 16 None: 12	Intermediate: 13 High: 3	Not: 8 Low: 11 None: 17	Not: 4 Low: 3 None: 7
McKeith Lewy body stage[b]	None: 16 Amyg. Pred.: 20	Transitional/Limbic: 3 Neocortical/Diffuse: 17	None: 23	None: 10	None: 12 Amyg. Pred.: 9	Transitional/Limbic: 1 Neocortical/Diffuse: 15	None: 17	None: 7

[a]Montine et al *Alzheimers Dement* 2016.
[b]McKeith et al *Neurology* 2005.
*p<0.05 UPenn v UCSD groups.
**p<0.05 ANOVA across UPenn cohort.
***p<0.05 ANOVA across UCSD cohort.
AD, Alzheimer disease; Amyg. Pred., amygdala-predominant; bvFTD, behavioral variant frontotemporal dementia; CBD, corticobasal degeneration; DLB, dementia with Lewy bodies; MCI, mild cognitive impairment; PDD, Parkinson disease with dementia; PPA, primary progressive aphasia; PSP, progressive supranuclear palsy; PSP-CBS, progressive supranuclear palsy-corticobasal syndrome; PSP-F, progressive supranuclear palsy with frontal lobe cognitive or behavioral presentation. PSP-P, Parkinsonism resembling idiopathic Parkinson disease, PSP-RS, progressive supranuclear palsy-Richardson syndrome; PSP-SL, progressive supranuclear palsy with speech/language disorder.
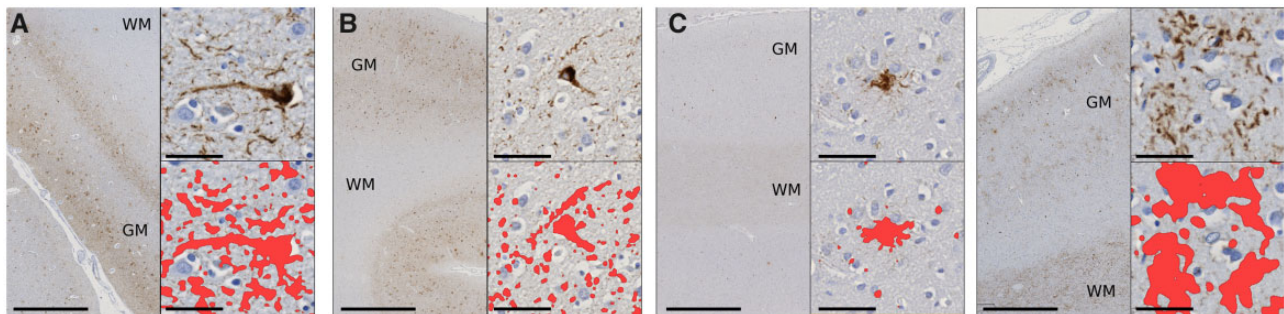
FIGURE 1. Tau histopathology. Representative images from AD **(A)**, LBD+tau **(B)**, PSP **(C)**, and CBD **(D)** cases. Low-magnification images (scale bar: 1 mm), show the higher grey matter pathology in AD and LBD+tau and higher degrees of white matter tau pathology in PSP and CBD. Higher-magnification images (scale bar: 40 μm) show neurofibrillary tangles in **(A)** and **(B)** with a tufted astrocyte in **(C)** and an astrocytic plaque in **(D)** with the digital detection overlay for the same image immediately below.

Digital measurements of pathological burdens were derived using the open source program QuPath (0.2.0m2 Belfast, Northern Ireland [62]) which calculated percent area occupied (%AO) for pathological tau accumulations (Fig. 1) (62). A single trained rater (DGC) selected grey matter and white matter regions of interest from the images derived at both sites using previously validated sampling methods (42, 43, 46, 63). Briefly, for grey matter annotations, a modified belt-transect method was used to select the longest region of representative parallel-oriented cortex using parallel lines drawn at the pial surface and grey-white junction to generate a rectangular region of interest (64). For white matter sampling, a rectangular area of deep white matter, away from U-fiber tracts was selected as regions of interest. Next random sampling was applied to each region using 175 μm^2 tiles with 70% dropout to reduce sampling bias (42, 43, 46, 63). Color deconvolution intensity thresholds were optimized per each staining run at each site by averaging values of red-blue-green color vectors and optimal minimal optical density values visually tuned from 3 to 5 representative slides per staining run (see Supplementary Data) (Fig. 1) as previously validated (46).

Red-blue-green vectors and optical density were recorded (see Supplementary Data). The same Gaussian sigma and downsample values were used for both sets of images (1 and 2, respectively). For both cohorts, the percent area-occupied by regional tau %AO (tau burden) was compared to gold-standard ordinal scores of pathological severity (0: none, 1: mild, 2: moderate, 3: severe) that were blindly assigned as previously described (42). For both cohorts, highly significant differences in tau burden were observed across traditional ordinal pathological severity scores (UPenn ANOVA: $F_{(244,3)}$: 430, $p < 0.001$. UCSD ANOVA: $F_{(137,3)} = 106$, $p < 0.001$) (Fig. 2).

Clinicopathological Correlations

We focused on the Folstein Mini Mental State exam (MMSE) score obtained closest to autopsy, as was sufficient data from both sites included in this study. Testing was administered by trained psychometrists. The MMSE closest to death was used to compare to the neocortical average grey matter and white matter tau burden as MMSE is a test of global cognitive function (time from testing to death: UPenn: 2.9 years±2.4 years, UCSD: 3.1 years±3.3 years). PSP and CBD groups from both institutions had <10 observations and were therefore excluded from this analysis (UPenn AD n = 35 (97%), LBD+tau n = 18 (90%), UCSD AD n = 20 (95%), LBD+tau n = 14 (88%)).

Statistical Analysis

Independent sample t-tests and χ^2 tests were used to assess differences in demographics and neuropathological features between groups as appropriate. Natural log transformation of %AO data allowed for the appropriate use of parametric tests. Linear mixed effects models, which account for repeated measures within cases, were used to investigate differences in regional tau burden in grey matter (GM) and white matter (WM) within AD, LBD+tau, PSP, and CBD groups using the following model: tau burden=region+random intercept for each disease group for white matter and grey matter. Reference regions were adjusted to account for all regional comparisons. Ratios of white matter to grey matter tau burden ([white matter tau burden]/[grey matter tau burden]) were calculated in each region and for the average of all regions for each patient for direct comparisons between disease groups using ANOVA with post hoc t-tests with Bonferroni correction. Linear regression was used to assess the relationship between the independent variable of neocortical average grey matter tau burden on the dependent variable white matter tau burden using grey matter×pathology group as an interaction term to assess for differential association grey and white matter tau burdens for each disease group. MMSE was compared to neocortical grey and white matter tau pathology using Pearson correlation.

RESULTS

Patient Demographics

One hundred fifty patients from UPenn and UCSD (UPenn n = 89, UCSD n = 61) were studied with minimal differences in demographics across disease groups (Table). The UPenn AD cohort had a younger age at death than the UCSD
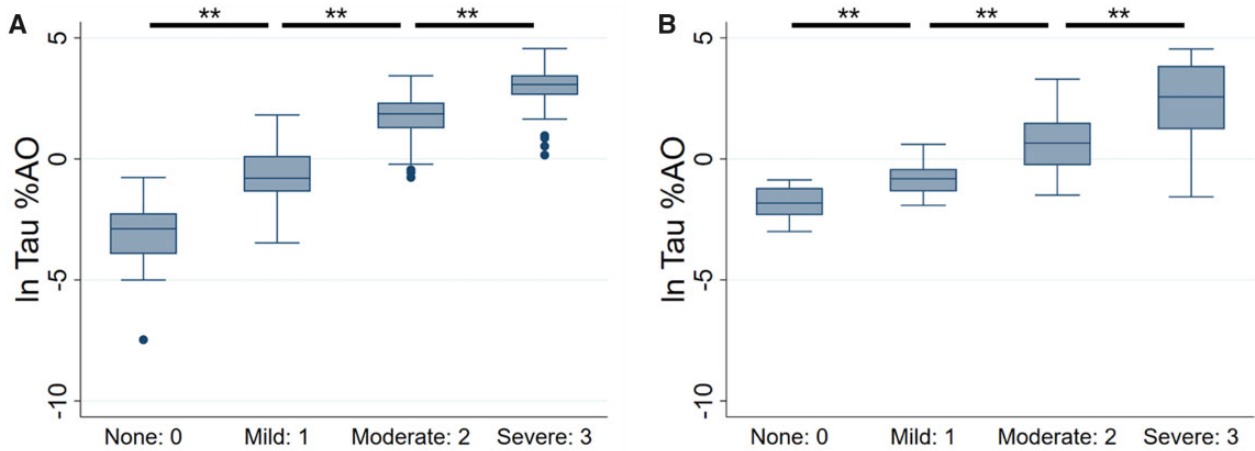
FIGURE 2. Semiquantitative ordinal scores and digital histological measurements. The relationship between traditional semiquantitative ordinal scores (0: none, 1: mild, 2: moderate, 3: severe) and the corresponding regional natural log tau % area occupied measurements (ln Tau %AO) in the cohort from University of Pennsylvania **(A)** and University of California San Diego **(B)**. Highly significant differences were observed between ordinal scores using ANOVA with post hoc Bonferroni corrected t-tests. **$p < 0.01$.
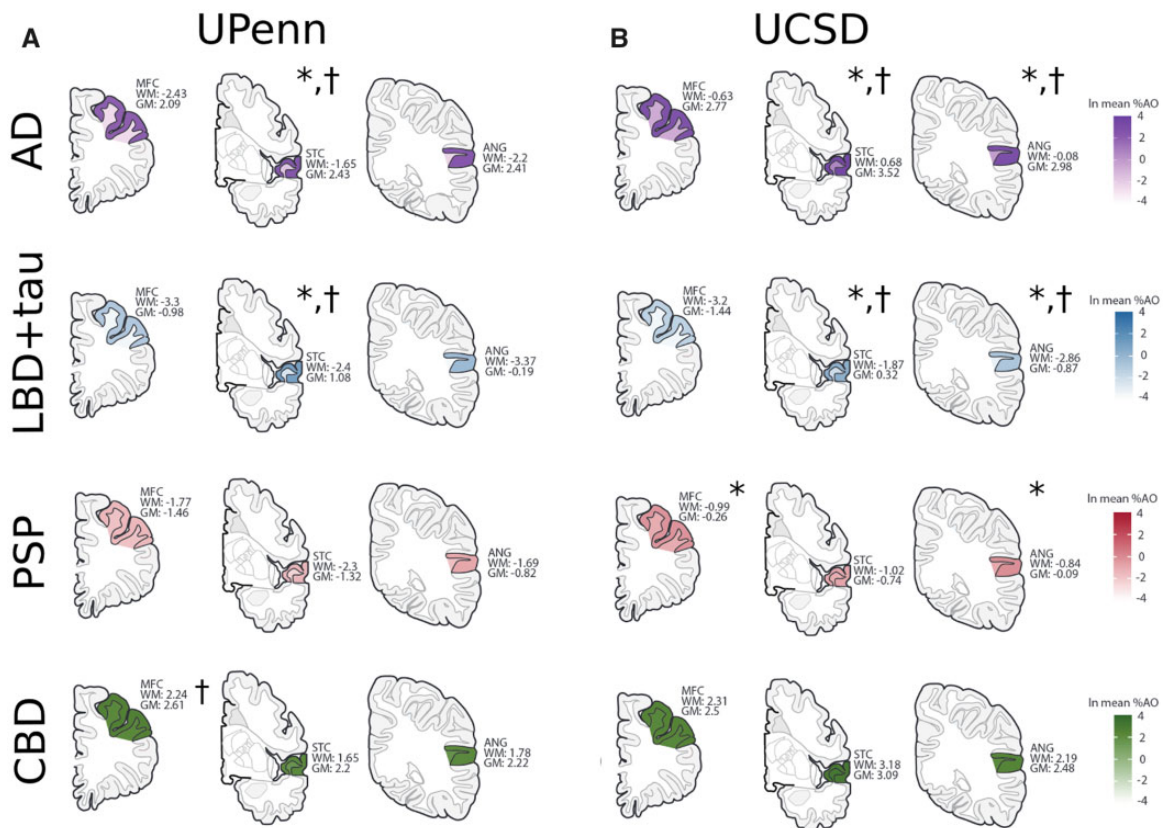
FIGURE 3. Heatmap of grey and white matter tau pathology. Regional grey matter (GM) and white matter (WM) tau burden (% area occupied: %AO) from UPenn **(A)** and UCSD **(B)** cohorts of AD (purple), LBD+tau (blue), PSP (red), and CBD (green). Similar patterns of GM and WM pathology are observed between institutions. Color gradient scale is the same for UPenn and UCSD and is shown at the right. *Grey matter tau burden with $p < 0.05$ compared to reference region using linear mixed effects models. †White matter tau burden with $p < 0.05$ compared to reference region using linear mixed effects models. Reference region for AD and LBD+tau: MFC, reference region for PSP and CBD: STC. See Supplementary Data for full comparisons.
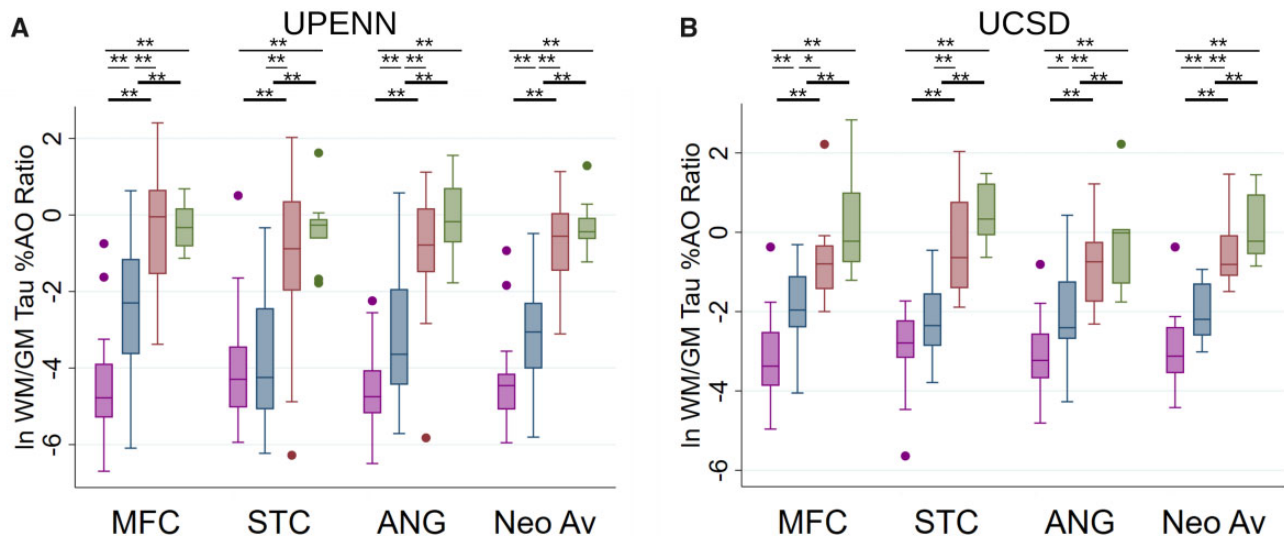
FIGURE 4. White matter/grey matter ratios of Tau burden in LBD and PSP. Box-plots depict the median, interquartile range, and range of the ratio of the natural log of white matter (WM) tau % area occupied (%AO) to grey matter (GM) tau % area occupied in AD (purple), LBD+tau (blue), PSP (red), and CBD (green) groups in the UPenn **(A)** and UCSD cohorts **(B)**. Relative white matter burden is consistently higher in PSP and CBD and in some regions LBD+tau has a higher WM/GM ratio than AD, likely driven by higher degrees of GM tau pathology in AD. *$p < 0.05$ and **$p < 0.01$ for post hoc Bonferroni corrected t-tests.

AD cohort ($p < 0.05$). Otherwise, there was no significant differences in sex, age at death or disease duration between LBD+tau and PSP groups or between UCSD and UPenn cohorts. The UPenn cohort had a higher proportion of AD cases with high degrees of AD neuropathological change than the UCSD cohort ($p = 0.02$) (Table).

Regional Grey Matter and White Matter Tau Pathology in AD, LBD+Tau, PSP, and CBD

Heatmaps for grey matter and white matter tau pathology for the pathological groups are shown in Figure 3. In both AD and LBD+tau, the highest degree of grey matter tau was found in the STC in both cohorts (UPenn: AD Wald $\chi^2=6.2$, $p = 0.03$; LBD+tau Wald $\chi^2=25.5$, $p < 0.001$. UCSD AD Wald $\chi^2=15.3$; $p < 0.001$; LBD+tau Wald $\chi^2=26.9$, $p < 0.001$). See Supplementary Data for full regional comparisons. In PSP, STC had the lowest degree of grey matter tau pathology in the UCSD cohort (Wald $\chi^2=8.0$, $p = 0.02$), but this did not reach statistical significance in the UPenn cohort. CBD had similar high-levels of grey matter tau pathology observed across regions sampled in both cohorts ($p > 0.05$) (Fig. 3 and Supplementary Data).

White matter tau burden in AD and LBD+tau was also greatest in STC for both cohorts (UPenn AD: Wald $\chi^2=18.5$, $p < 0.001$; LBD+tau Wald $\chi^2=6.23$, $p = 0.04$. UCSD AD: Wald $\chi^2=45.0$, $p < 0.001$; LBD+tau Wald $\chi^2=11.9$, $p = 0.003$) while region was not a significant factor in PSP, suggesting similar relatively high burden among white matter regions sampled ($p > 0.3$) (Fig. 3 and Supplementary Data). CBD WM pathology in the UPenn cohort was highest in the MFC (MFC v STC $p = 0.02$) but this was not observed in the UCSD cohort. An analysis controlling for disease duration,

sex, and age at death did not change any of the relationships observed above (data not shown).

Comparative Burden of Regional Grey Matter and White Matter Tau Pathology

Since varied morphology of tau inclusions between tauopathies can influence measurements using these methods we calculated a ratio of tau pathology in white matter over grey matter for direct comparisons between groups of the relative burden of pathology and found overall an increased white matter/grey matter ratio across the diseases studied with AD < LBD+tau < the 4R tauopathies (PSP and CBD); although, a larger difference was noted between 3R/4R tauopathies and 4R tauopathies (Fig. 4 and Supplementary Data).

Association of Grey Matter and White Matter Tau Pathology

There were significant correlations between GM and WM neocortical average tau burdens in all diseases studied in both cohorts ($R^2=0.43–0.79$, $p = 0.04$ to <0.001, Supplementary Data). Because the slope of the association between grey matter tau and white matter tau appeared to be greater for PSP than the other disease groups, we used a linear regression model with an interaction term for disease group×grey matter tau burden to test for differences in the associations of grey matter and white matter tau burden between the diseases. The slopes of the grey and white matter tau associations were significantly less in AD and LBD+tau than PSP in both cohorts (UPenn: AD $p = 0.002$, LBD+tau $p < 0.001$. UCSD: AD, $p = 0.02$, LBD+tau $p = 0.004$) suggesting that for every unit of grey tau pathology increase there was a higher amount of
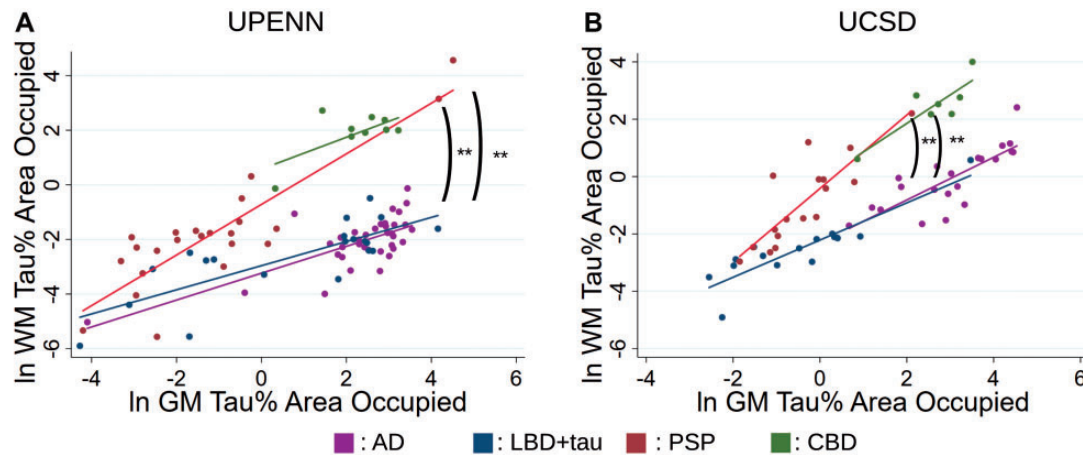
FIGURE 5. White matter and grey matter Tau correlations. Scatter plots and lines of best fit depict the relationship between the grey matter (GM) neocortical average tau % area occupied and white matter (WM) neocortical average tau % area occupied (%AO) in AD (purple) LBD+tau (blue), PSP (red), and CBD (green). Highly significant correlations are noted for all disease groups in both the UPenn **(A)** and UCSD **(B)** cohorts. The interaction term of pathology group* grey matter tau %AO finds for each unit GM tau pathology added, there is a significantly greater amount of WM pathology noted in PSP than AD or PSP compared to LBD+tau as well. This interaction was not found for CBD compared to AD or LBD+tau. **$p < 0.01$.

white matter tau pathology increase seen in PSP than in AD or LBD+tau. CBD grey matter tau did not have an increased slope compared to the 3R/4R tauopathies in either cohort in this study (Fig. 5 and Supplementary Data).

Clinicopathological Correlations

Significant negative correlations were observed with in AD and LBD+tau neocortical average grey matter tau burden and performance on the MMSE (UPenn AD $R = -0.44$, $p = 0.008$; UCSD AD $R = -0.52$, $p = 0.02$. UPenn LBD+tau $R = -0.45$, $p = 0.06$; UCSD LBD+tau $R = -0.70$, $p = 0.006$). Some trend level associations were observed between neocortical white matter tau burden and MMSE performance as well (UPenn AD $R = -0.29$, $p = 0.08$; UCSD AD $R = -0.32$, $p = 0.2$; UPenn AD $R = -0.44$, $p = 0.06$; UCSD LBD+tau $R = -0.55$, $p = 0.04$) (Fig. 6 and Supplementary Data).

DISCUSSION

In this study of tau pathology in AD, LBD, PSP, and CBD using validated digital histological methods across 2 centers, we report several findings of interest that highlight different patterns and relationships of grey and white matter tau which may have relevance for mechanisms of propagation. We observe that the temporal lobe has the highest degree of GM and WM tau pathology in AD and LBD+tau, while the relative burden of WM tau pathology is overall higher in the PSP and CBD groups. These observations are reflections of the progression of AD-related tau pathology and tau pathology distribution in different cell populations in 4R tauopathies, but this study extends this knowledge in using quantitative digital image analysis methods across 2 institutions which allow for novel statistical modeling to explore these relationships. We find a stronger association between the burden of grey matter tau and adjacent white matter tau pathology in the PSP com-

pared to the 3R/4R groups. Together these results suggest white matter tau pathology may be an important contributor to the spread of PSP tauopathy. Importantly, these findings were robustly replicated across both institutional cohorts studied. Our data also have important implications for models of disease progression in the human brain and provide new methodology to harmonize digital pathological assessment across centers.

Tau pathology has been extensively studied in PSP. The specific species of tau aggregates include 4R isoforms and occur in astroglia (tufted astrocytes), oligodendroglia (coiled bodies), and neuronal cell populations (globose tangles) throughout regions of the brainstem, basal ganglia, and neocortical areas (38, 65, 66). The cortical distribution of tau pathology may partially relate to clinical cognitive dysfunction, as not only patients with classical Richardson syndrome (PSP-RS), but also those with clinical syndromes of behavioral variant frontotemporal dementia, corticobasal syndrome, or primary progressive aphasia may also harbor PSP pathology at autopsy (3, 38, 67). Indeed, a histopathological staging system for PSP has recently been proposed which finds similar high burden of deep grey matter and brainstem pathology across clinical subgroups with varying cortical involvement most prominent in motor cortex and frontoparietal lobes with relative sparing of the temporal cortex (38). Here, we found similar results of high burdens of grey matter tau pathology throughout our regions sampled, most notably in ANG which was greater than temporal cortex in the UCSD cohort. White matter tau pathology was similarly distributed across the 3 cortical regions we examined in both cohorts, but there was relatively lower burden in STC. Focused studies of white matter tau in PSP are less common, although oligodendroglial tau progression is accounted for in the recent proposed staging system (38). We recently examined regional white matter tau in PSP tauopathy associated with clinical frontotemporal dementia and found relatively high burden of tau in white mat-
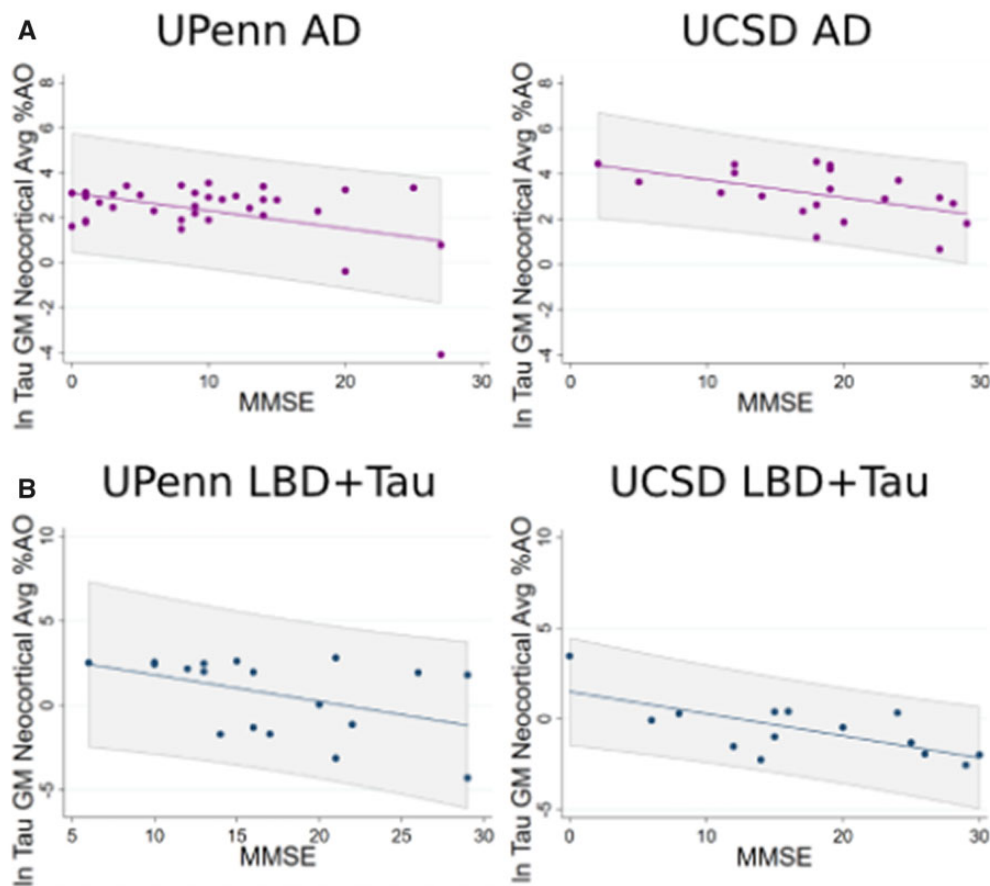
FIGURE 6. Neocortical grey matter Tau and cognition. Scatter plots and lines of best fit with shaded standard deviation predictions depict the relationship between neocortical grey matter tau burden and performance on the Folstein Mini Mental State exam in AD and LBD+tau. Significant negative correlations were found in each disease in both cohorts (p < 0.05).

ter of ANG with relative sparing of STC (68). Others have examined deep white matter tau in PSP and other tauopathies and found relative divergent distributions in those with dementia compared to motor phenotypes (69). Moreover, white matter disease in vivo has been linked to clinical features in PSP (35, 70, 71). Thus, the prominent white matter tau pathology in PSP may play an important role in the propagation of tau in the cerebrum and expression of clinical symptoms. In CBD, tau pathology primarily occurs in astrocytic plaques, coiled bodies in oligodendroglial cells and in neurons (72); however, no unified staging system related to CBD pathology has been proposed to date. Some studies would suggest more cortical involvement in CBD than PSP relative to brainstem pathology (73). While both CBD and PSP are 4R tauopathies, there are distinct ultrastructural differences in tau conformations that have been shown by electron microscopy experiments that may have relevance to pathogenesis (74, 75). In this study, CBD had the highest degrees of white matter tau pathology, in some cases with higher burdens in white matter than grey matter in the same regions. This observation may lead to a ceiling effect of some of these analyses which, along with a lower number of cases, may have led to some of the differences in grey matter-white matter correlations between

institutions and when comparing the grey matter-white matter associations in CBD to the other diseases studied here. Future directed studies of larger cohorts of CBD subjects will be of interest.

While in AD 3R/4R tau accumulations primarily in neurofibrillary tangles are a pathological hallmark of the disease and progress in a largely stereotypic fashion in typical amnestic AD (37), in LBD, 3R/4R AD-related tau-positive neurofibrillary tangles and AD neuropathological changes sufficient for a secondary pathological diagnosis of AD are observed in approximately 50% of autopsy cohorts (PD without dementia ~10%, PDD ~30%–50%; and DLB ~70%) (6, 8, 10, 14, 76, 77). The presence of AD copathology in LBD is associated with faster time to dementia in PD, decreased overall survival but also specific motor and cognitive profiles (6, 13, 17, 18, 42, 55, 78). The greatest grey matter tau burden was observed in the temporal lobes of LBD+tau subjects which is consistent with the traditional neocortical spread of AD tau-related changes and has been shown in several neuropathological and imaging studies (26, 28, 31, 37, 42, 45). Of interest though is that there are multiple pathological and imaging studies that suggest a temporo-parietal focus with relative hippocampal sparing of tau pathology in LBD that may differ from patterns

seen in AD (26, 28, 31, 41, 42, 45). This has clinical relevance for language features of naming difficulties and episodic memory deficits less commonly found in LBD but recently linked to AD tau pathology and biomarkers (12, 17, 42, 79, 80). Tau-positive inclusions in white matter in LBD are understudied although their presence has been documented in AD (81). Here we find similar tau pathology in WM as previously described in AD, largely restricted to axonal threads in LBD+Tau. Imaging studies, predominantly using diffusion tensor imaging, have shown decreases in WM integrity in LBD and PSP in cross-sectional and longitudinal studies in unique patterns (70, 71, 82–84). It is interesting to hypothesize that axonal WM tau pathology in AD and LBD may be more closely linked to neuronal degeneration and tau NFTs in degenerating neurons, as compared to PSP which has additional glial tau in white matter.

In many instances, patients with overlapping motor phenotypes especially who are early in their disease course can be difficult to differentiate (67), but the continued study of tau-directed imaging and biofluid biomarkers offers the potential future ability to differentiate these patients using molecularly specific methods (25, 27, 30, 31, 45, 85). A detailed understanding of the neuropathological distribution of pathology can help in interpreting these studies as tau-directed imaging biomarkers continue their development and understanding for their relevance to different tau species increases. Using digital measures, we could directly compare the relative grey and white matter tau burden in AD, LBD+tau, PSP, and CBD. We found overall white matter tau pathology is more severe in PSP and CBD than AD and LBD+tau groups. Indeed, white matter astroglial and oligodendroglial pathology is a core neuropathological feature of PSP and CBD and our data suggests the development of white matter-directed imaging biomarkers may aid in differentiating these patients (38, 65, 70, 71, 86, 87). Using these digital histological methods, we were able to demonstrate a differential relationship between grey and white tau pathology in PSP and the other diseases where there was a correspondingly higher amount of white tau pathology increase for each unit of grey matter tau pathology increase in PSP compared to LBD+tau and AD. These data suggest white matter glial tau in PSP may be influential in cortical spread of PSP in a manner distinct from tau in AD and LBD. There was not a statistically different relationship observed in the CBD cases when compared to the 3R/4R cases and we speculate that this may be due to low number of cases or a ceiling effect of relatively high grey and white matter tau burdens in CBD. Interestingly, novel animal studies have suggested that different tauopathy strains have unique transmission patterns and ability to affect neuronal, oligodendroglial, and astrocytic cell populations differentially (38, 88–91). In PSP, some studies suggest that tau pathology originates in neurons and then spreads to glial cells and others show that oligodendroglial pathology can propagate in the absence of neuronal tau pathology (38, 88, 89). Detailed study may also inform future hypothesis of models of disease pathogenesis and spread within the human brain.

Traditional neuropathological assessments often rely on semiquantitative ordinal scores and scales that tend to emphasize topography over severity of pathology. While widely adopted, there can be inter-rater variability in assessing cases, and the semiquantitative methodology limits statistical analyses (92, 93). Digital image analysis in neuropathological tissues can offer a finely grained, parametric assessments, with good intra and inter-rater reliability within single centers that allow for greater power to examine patterns of disease but also clinicopathological and biomarker-pathological correlations (41–43, 45, 48, 49); however, there is limited data to determine if methods are scalable for multisite studies. This is particularly pertinent given the potential influence of local histological preparation techniques, immunostaining methods, and image acquisition methods and file types on these types of analyses (46). In this study we controlled for many of these variables using the same commercially available reagents, the same immunostaining protocol optimized for each site with the same rater drawing ROIs using an open source digital histological analysis platform (QuPath [62]). Some sources of variability remained, including the use of different slide scanners and file types that were analyzed. Despite these sources of variability, we observed very consistent results of grey and white matter tau pathology across both cohorts that were studied that recapitulate known patterns of disease but also raise novel findings.

There are limitations to this study. While our sample size was comparable to standard histopathological studies, it was relatively small to capture the full clinical spectrum of PSP and LBD with sufficient numbers to perform detailed exploration of PD dementia versus DLB and PSP-RS versus other forms of PSP clinical syndromes. There was not perfect agreement in the results of the 2 cohorts with grey tau in the PSP group from UCSD having some regional differences that did not reach statistical significance in the UPenn cohort. This does not appear to be due to demographics or PSP phenotypes given that subanalyses were performed controlling for disease duration, age at death, and sex, as well as restricting analyses to cases with the PSP-Richardson Syndrome phenotype. Further study is needed, but this may reflect pathological heterogeneity within PSP tauopathy that need to be explored in larger multicentered cohorts. There were small differences in the distribution of tau in AD cases between the UPenn and UCSD cohorts, which is likely due to the UCSD cohort having a larger amount of cases with an intermediate stage of ADNC, allowing for greater likelihood of being able to observe differences between regions in their tau burdens. Importantly, our digital analyses found similar effect sizes between tissue obtained and processed at each center, suggesting digital measures of histopathology are feasible for large-scale multi-center cohorts. Indeed, we were careful to control for many preanalytical histopathological and imaging factors, but future work is needed to establish detailed standard operating procedures to coordinate large-scale multicentered harmonized efforts. Nonetheless, our initial work is important to help develop these approaches. The current digital method applied here assesses for the percent area occupied by total tau pathology. Future efforts will focus on more refined efforts using machine learning image analysis techniques to differentiate different inclusion types for subsequent deep pathological phenotyping (49, 94, 95) and the clinical correlates of regional cellular tau pathology as measured by these more granular

methods. With these caveats in mind, in this multicentered study using digital histological methods carefully controlling for staining and image analysis techniques, we observe patterns of GM and WM tau pathology in AD, LBD+tau, PSP, and CBD, that conform to prior reports using traditional neuropathological methods but also add new observations about the relationship between grey and white matter tau accumulations in these diseases which would not be possible without using these methods. The use of digital histological methods in controlled studies may offer the ability to perform detailed, well-powered, studies across multiple sites for the continued study of clinicopathological and biomarker pathological associations in neurodegenerative disease.

DATA AVAILABILITY

Datasets will be made available upon reasonable request.

REFERENCES

1. Postuma RB, Berg D, Stern M, et al. MDS clinical diagnostic criteria for Parkinson's disease. Mov Disord 2015;30:1591–601
2. McKhann GM, Knopman DS, Chertkow H, et al. The diagnosis of dementia due to Alzheimer's disease: Recommendations from the National Institute on Aging-Alzheimer's Association workgroups on diagnostic guidelines for Alzheimer's disease. Alzheimer's Dement 2011;7:263–9
3. Höglinger GU, Respondek G, Stamelou M, et al.; Movement Disorder Society-Endorsed PSP Study Group. Clinical diagnosis of progressive supranuclear palsy: The movement disorder society criteria. Mov Disord 2017;32:853–64
4. Armstrong MJ, Litvan I, Lang AE, et al. Criteria for the diagnosis of corticobasal degeneration. Neurology 2013;80:496–503
5. Jellinger KA, Seppi K, Wenning GK, et al. Impact of coexistent Alzheimer pathology on the natural history of Parkinson's disease. J Neural Transm 2002;109:329–39
6. Irwin DJ, Grossman M, Weintraub D, et al. Neuropathological and genetic correlates of survival and dementia onset in synucleinopathies: A retrospective analysis. Lancet Neurol 2017;16:55–65
7. Marui W, Iseki E, Kato M, et al. Pathological entity of dementia with Lewy bodies and its differentiation from Alzheimer's disease. Acta Neuropathol 2004;108:121–8
8. Irwin DJ, White MT, Toledo JB, et al. Neuropathologic substrates of Parkinson disease dementia. Ann Neurol 2012;72:587–98
9. Smith C, Malek N, Grosset K, et al. Neuropathology of dementia in patients with Parkinson's disease: A systematic review of autopsy studies. J Neurol Neurosurg Psychiatry 2019;90:1234–43
10. Dugger BN, Adler CH, Shill HA, et al.; Arizona Parkinson's Disease Consortium. Concomitant pathologies among a spectrum of parkinsonian disorders. Parkinsonism Relat Disord 2014;20:525–9
11. Armstrong RA, Lantos PL, Cairns NJ. Overlap between neurodegenerative disorders. Neuropathology 2005;25:111–24
12. Ryman SG, Yutsis M, Tian L, et al. Cognition at each stage of Lewy body disease with co-occurring Alzheimer's disease pathology. J Alzheimers Dis 2021;80:1243–56
13. Dugger BN, Boeve BF, Murray ME, et al. Rapid eye movement sleep behavior disorder and subtypes in autopsy-confirmed dementia with Lewy bodies. Mov Disord 2012;27:72–8
14. Halliday G, Hely M, Reid W, et al. The progression of pathology in longitudinally followed patients with Parkinson's disease. Acta Neuropathol 2008;115:409–15
15. Compta Y, Parkkinen L, O'Sullivan SS, et al. Lewy-and Alzheimer-type pathologies in Parkinson's disease dementia: Which is more important? Brain 2011;134:1493–505
16. Howlett DR, Whitfield D, Johnson M, et al. Regional multiple pathology scores are associated with cognitive decline in Lewy body dementias. Brain Pathol 2015;25:401–8
17. Peavy GM, Edland SD, Toole BM, et al. Phenotypic differences based on staging of Alzheimer's neuropathology in autopsy-confirmed dementia with Lewy bodies. Parkinsonism Relat Disord 2016;31:72–8
18. Sabbagh MN, Adler CH, Lahti TJ, et al. Parkinson disease with dementia: Comparing patients with and without Alzheimer pathology. Alzheimer Dis Assoc Disord 2009;23:295–7
19. Lopez OL, Becker JT, Kaufer DI, et al. Research evaluation and prospective diagnosis of dementia with Lewy bodies. Arch Neurol 2002;59:43–6
20. Merdes AR, Hansen LA, Jeste DV, et al. Influence of Alzheimer pathology on clinical diagnostic accuracy in dementia with Lewy bodies. Neurology 2003;60:1586–90
21. Kraybill ML, Larson EB, Tsuang DW, et al. Cognitive differences in dementia patients with autopsy-verified AD, Lewy body pathology, or both. Neurology 2005;64:2069–73
22. McKeith IG, Boeve BF, Dickson DW, et al. Diagnosis and management of dementia with Lewy bodies Fourth consensus report of the DLB Consortium. Neurology 2017;89:88–100
23. Josephs KA, Petersen RC, Knopman DS, et al. Clinicopathologic analysis of frontotemporal and corticobasal degenerations and PSP. Neurology 2006;66:41–8
24. Fleisher AS, Pontecorvo MJ, Devous MD, et al.; A16 Study Investigators. Positron emission tomography imaging with [18F] flortaucipir and postmortem assessment of Alzheimer disease neuropathologic changes. JAMA Neurol 2020;77:829–39
25. Ossenkoppele R, Rabinovici GD, Smith R, et al. Discriminative accuracy of [18F] flortaucipir positron emission tomography for Alzheimer disease vs other neurodegenerative disorders. Jama 2018;320:1151–62
26. Smith R, Scholl M, Londos E, et al. (18)F-AV-1451 in Parkinson's disease with and without dementia and in dementia with Lewy bodies. Sci Rep 2018;8:4717
27. Smith R, Schain M, Nilsson C, et al. Increased basal ganglia binding of 18 F-AV-1451 in patients with progressive supranuclear palsy. Mov Disord 2017;32:108–14
28. Lee SH, Cho H, Choi JY, et al. Distinct patterns of amyloid-dependent tau accumulation in Lewy body diseases. Mov Disord 2018;33:262–72
29. Gomperts SN, Locascio JJ, Makaretz SJ, et al. Tau positron emission tomographic imaging in the Lewy body diseases. JAMA Neurol 2016; 73:1334–41
30. Lowe VJ, Lundt ES, Albertson SM, et al. Tau-positron emission tomography correlates with neuropathology findings. Alzheimers Dement 2020;16:561–71
31. Kantarci K, Lowe VJ, Boeve BF, et al. AV-1451 tau and β-amyloid positron emission tomography imaging in dementia with Lewy bodies. Ann Neurol 2017;81:58–67
32. Ishiki A, Harada R, Okamura N, et al. Tau imaging with [18 F]THK-5351 in progressive supranuclear palsy. Eur J Neurol 2017;24:130–6
33. Hsu JL, Chen SH, Hsiao IT, et al. 18F-THK5351 PET imaging in patients with progressive supranuclear palsy: Associations with core domains and diagnostic certainty. Sci Reports 2020;10:1–10
34. Tezuka T, Takahata K, Seki M, et al. Evaluation of [18F]PI-2620, a second-generation selective tau tracer, for assessing four-repeat tauopathies. Brain Commun 2021;3:fcab190
35. Spotorno N, Hall S, Irwin DJ, et al. Diffusion tensor MRI to distinguish progressive supranuclear palsy from a-synucleinopathies. Radiology 2019;293:646–53
36. Zhang Y, Walter R, Ng P, et al. Progression of microstructural degeneration in progressive supranuclear palsy and corticobasal syndrome: A longitudinal diffusion tensor imaging study. PLoS One 2016;11:e0157218
37. Braak H, Alafuzoff I, Arzberger T, et al. Staging of Alzheimer disease-associated neurofibrillary pathology using paraffin sections and immunocytochemistry. Acta Neuropathol 2006;112:389–404
38. Kovacs G, Lukic MJ, Irwin DJ, et al. Distribution patterns of tau pathology in progressive supranuclear palsy. Acta Neuropathol 2020;140: 99–119
39. Muller CM, de Vos RA, Maurage CA, et al. Staging of sporadic Parkinson disease-related alpha-synuclein pathology: Inter- and intra-rater reliability. J Neuropathol Exp Neurol 2005;64:623–8
40. Chui HC, Tierney M, Zarow C, et al. Neuropathologic diagnosis of Alzheimer disease: Interrater reliability in the assessment of senile plaques and neurofibrillary tangles. Alzheimer Dis Assoc Disord 1993;7:48–54
41. Walker L, McAleese KE, Thomas AJ, et al. Neuropathologically mixed Alzheimer's and Lewy body disease: Burden of pathological protein

aggregates differs between clinical phenotypes. Acta Neuropathol 2015; 129:729–48

42. Coughlin D, Xie SX, Liang M, et al. Cognitive and pathological influences of tau pathology in Lewy body disorders. Ann Neurol 2019;85: 259–71

43. Coughlin DG, Ittyerah R, Peterson C, et al. Hippocampal subfield pathologic burden in Lewy body diseases vs. Alzheimer's disease. Neuropathol Appl Neurobiol 2020;46:707–21

44. Spotorno N, Coughlin DG, Olm CA, et al. Tau pathology associates with in vivo cortical thinning in Lewy body disorders. Ann Clin Transl Neurol 2020;7:2342–55

45. Coughlin DG, Phillips JS, Roll E, et al.; Alzheimer's Disease Neuroimaging Initiative. Multimodal in vivo and post-mortem assessments of tau in Lewy body disorders. Neurobiol Aging 2020;96:137–47

46. Giannini LAA, Xie SX, McMillan CT, et al. Divergent patterns of TDP-43 and tau pathologies in primary progressive aphasia. Ann Neurol 2019; 85:630–43

47. Irwin DJ, McMillan CT, Xie SX, et al. Asymmetry of post-mortem neuropathology in behavioural-variant frontotemporal dementia. Brain 2018;141:288–301

48. Neltner JH, Abner EL, Schmitt FA, et al. Digital pathology and image analysis for robust high-throughput quantitative assessment of Alzheimer disease neuropathologic changes. J Neuropathol Exp Neurol 2012;71: 1075–85

49. Abner EL, Neltner JH, Jicha GA, et al. Diffuse amyloid-β plaques, neurofibrillary tangles, and the impact of APOE in elderly persons' brains lacking neuritic amyloid plaques. J Alzheimers Dis 2018;64:1307–24

50. Xie SX, Baek Y, Grossman M, et al. Building an integrated neurodegenerative disease database at an academic health center. Alzheimers Dement 2011;7:e84–93

51. Toledo JB, Van Deerlin VM, Lee EB, et al. A platform for discovery: The University of Pennsylvania Integrated Neurodegenerative Disease Biobank. Alzheimers Dement 2014;10:477–84.e1

52. Adamowicz DH, Roy S, Salmon DP, et al. Hippocampal alpha-synuclein in dementia with Lewy bodies contributes to memory impairment and is consistent with spread of pathology. J Neurosci 2017;37:1675–84

53. Thal DR, Rub U, Orantes M, et al. Phases of A beta-deposition in the human brain and its relevance for the development of AD. Neurology 2002;58:1791–800

54. Mirra SS, Heyman A, McKeel D, et al. The Consortium to Establish a Registry for Alzheimer's Disease (CERAD). Part II. Standardization of the neuropathologic assessment of Alzheimer's disease. Neurology 1991;41:479–86

55. McKeith IG, Dickson DW, Lowe J, et al.; Consortium on DLB. Diagnosis and management of dementia with Lewy bodies: Third report of the DLB Consortium. Neurology 2005;65:1863–72

56. Nelson PT, Dickson DW, Trojanowski JQ, et al. Limbic-predominant age-related TDP-43 encephalopathy (LATE): Consensus Working Group report. Brain 2019;142:1503–27

57. Kovacs GG, Xie SX, Robinson JL, et al. Sequential stages and distribution patterns of aging-related tau astrogliopathy (ARTAG) in the human brain. Acta Neuropathol Commun 2018;6:50

58. Montine TJ, Phelps CH, Beach TG, et al.; Alzheimer's Association. National Institute on Aging-Alzheimer's Association guidelines for the neuropathologic assessment of Alzheimer's disease: A practical approach. Acta Neuropathol 2012;123:1–11

59. Emre M, Aarsland D, Brown R, et al. Clinical diagnostic criteria for dementia associated with Parkinson's disease. Mov Disord 2007;22: 1689–707; quiz 1837

60. Dickson DW, Ahmed Z, Algom AA, et al. Neuropathology of variants of progressive supranuclear palsy. Curr Opin Neurol 2010;23:394–400

61. Dickson DW, Kouri N, Murray ME, et al. Neuropathology of frontotemporal lobar degeneration-tau (FTLD-Tau). J Mol Neurosci 2011;45: 384–9

62. Bankhead P, Loughrey MB, Fernández JA, et al. QuPath: Open source software for digital pathology image analysis. Sci Rep 2017;7:16878

63. Armstrong RA. Quantifying the pathology of neurodegenerative disorders: Quantitative measurements, sampling strategies and data analysis. Histopathology 2003;42:521–9

64. Irwin DJ, Brettschneider J, McMillan CT, et al. Deep clinical and neuropathological phenotyping of Pick disease. Ann Neurol 2016;79:272–87

65. Hauw J-J, Daniel SE, Dickson D, et al. Preliminary NINDS neuropathologic criteria for Steele-Richardson-Olszewski syndrome (progressive supranuclear palsy). Neurology 1994;44:2015–9

66. Williams DR, Holton JL, Strand C, et al. Pathological tau burden and distribution distinguishes progressive supranuclear palsy-parkinsonism from Richardson's syndrome. Brain 2007;130:1566–76

67. Respondek G, Stamelou M, Kurz C, et al.; Movement Disorder Society-endorsed PSP Study Group. The phenotypic spectrum of progressive supranuclear palsy: A retrospective multicenter study of 100 definite cases. Mov Disord 2014;29:1758–66

68. Giannini LAA, Peterson C, Ohm D, et al. Frontotemporal lobar degeneration proteinopathies have disparate microscopic patterns of white and grey matter pathology. Acta Neuropathol Commun 2021;9:1–19

69. Kim E-J, Hwang J-HL, Gaus SE, et al. Evidence of corticofugal tau spreading in patients with frontotemporal dementia. Acta Neuropathol 2020;139:27–43

70. Sintini I, Schwarz CG, Senjem ML, et al. Multimodal neuroimaging relationships in progressive supranuclear palsy. Parkinsonism Relat Disord 2019;66:56–61

71. Saini J, Bagepally BS, Sandhya M, et al. In vivo evaluation of white matter pathology in patients of progressive supranuclear palsy using TBSS. Neuroradiol 2012;54:771–80

72. Lee SE, Rabinovici GD, Mayo MC, et al. Clinicopathological correlations in corticobasal degeneration. Ann Neurol 2011;70:327–40

73. Mimuro M, Yoshida M. Chameleons and mimics: Progressive supranuclear palsy and corticobasal degeneration. Neuropathology 2020;40: 57–67

74. Zhang W, Tarutani A, Newell KL, et al. Novel tau filament fold in corticobasal degeneration, a four-repeat tauopathy. Nature 2020;580:283–7

75. Shi Y, Zhang W, Yang Y, et al. Structure-based classification of tauopathies. Nature 2021;598:359–63

76. Marui W, Iseki E, Nakai T, et al. Progression and staging of Lewy pathology in brains from patients with dementia with Lewy bodies. J Neurol Sci 2002;195:153–9

77. Jellinger KA, Attems J. Prevalence and impact of vascular and Alzheimer pathologies in Lewy body disease. Acta Neuropathol 2008;115: 427–36

78. Coughlin DG, Hurtig HI, Irwin DJ. Pathological influences on clinical heterogeneity in Lewy body diseases. Mov Disord 2020;35:5–19

79. Cholerton BA, Poston KL, Yang L, et al. Semantic fluency and processing speed are reduced in non-cognitively impaired participants with Parkinson's disease. J Clin Exp Neuropsychol 2021;43:469–80

80. Howard E, Irwin DJ, Rascovsky K, et al. Cognitive profile and markers of Alzheimer disease-type pathology in patients with Lewy body dementias. Neurology 2021;96:e1855–64

81. Iseki E, Togo T, Suzuki K, et al. Dementia with Lewy bodies from the perspective of tauopathy. Acta Neuropathol 2003;105:265–70

82. Taylor KI, Sambataro F, Boess F, et al. Progressive decline in gray and white matter integrity in de novo Parkinson's disease: An analysis of longitudinal Parkinson progression markers initiative diffusion tensor imaging data. Front Aging Neurosci 2018;10:318

83. Zanigni S, Calandra-Buonaura G, Manners DN, et al. Accuracy of MR markers for differentiating progressive supranuclear palsy from Parkinson's disease. Neuroimage Clin 2016;11:736–42

84. Kantarci K, Avula R, Senjem ML, et al. Dementia with Lewy bodies and Alzheimer disease. Neurology 2010;74:1814–21

85. Irwin DJ, Xie SX, Coughlin D, et al. CSF tau and amyloid-beta predict cerebral synucleinopathy in autopsied Lewy body disorders. Neurology 2018;90:e1038–46

86. Whitwell JL, Tosakulwong N, Botha H, et al. Brain volume and flortaucipir analysis of progressive supranuclear palsy clinical variants. Neuroimage Clin 2020;25:102152

87. Whitwell JL, Avula R, Master A, et al. Disrupted thalamocortical connectivity in PSP: A resting-state fMRI, DTI, and VBM study. Parkinsonism Relat Disord 2011;17:599–605

88. Ferrer I, García MA, Carmona M, et al. Involvement of oligodendrocytes in tau seeding and spreading in tauopathies. Front Aging Neurosci 2019; 11:112

89. Narasimhan S, Changolkar L, Riddle DM, et al. Human tau pathology transmits glial tau aggregates in the absence of neuronal tau. J Exp Med 2020;217:e20190783

90. Walker LC. Glial tauopathy: Neurons optional? J Exp Med 2020;217: e20191915
91. He Z, McBride JD, Xu H, et al. Transmission of tauopathy strains is independent of their isoform composition. Nat Commun 2020;11: 1–18
92. Beach TG, Corbille A-G, Letournel F, et al. Multicenter assessment of immunohistochemical methods for pathological alpha-synuclein in sigmoid colon of autopsied Parkinson's disease and control subjects. J Parkinsons Dis 2016;6:761–70
93. Montine TJ, Monsell SE, Beach TG, et al. Multisite assessment of NIA-AA guidelines for the neuropathologic evaluation of Alzheimer's disease. Alzheimer's. Alzheimers Dement 2016;12:164–9
94. Koga S, Ikeda A, Dickson DW. Deep learning-based model for diagnosing Alzheimer's disease and tauopathies. Neuropathol Appl Neurobiol 2022;48:e12759
95. Koga S, Ghayal NB, Dickson DW. Deep learning-based image classification in differentiating tufted astrocytes, astrocytic plaques, and neuritic plaques. J Neuropathol Exp Neurol 2021;80:306–12